Journal of Aeronautics, Astronautics and Aviation, Vol. 57, No. 3S, pp. 593 – 603 (2025)
https://doi.org/10.6125/JoAAA.202505_57(3S).32

Induction Heating Method for Thermomechanical Study of NiTi Shape Memory Alloy Wire

Sivasanghari Karunakaran and Dayang Laila Abang Abdul Majid *

Department of Aerospace Engineering, Faculty of Engineering, Universiti Putra Malaysia, 43400 Serdang, Selangor, Malaysia.

ABSTRACT

Thermo-mechanically responsive shape memory alloys (SMA) with high strain generation have shown remarkable properties particularly, the shape memory effect when use as an actuator. However, in practical applications, it is difficult to characterize the shape memory behaviour due to the complex coupling interaction between load and temperature that resulted in dynamic nonlinear hysteresis. The actuation capability of SMA is depending on the heat control mechanism of SMA. Herein, a comprehensive study is established for Flexinol NiTi wire using induction heating and compared to established data to reveal the feasibility of induction heating for SMA thermomechanical characterization. A precise regulated heat control chamber utilizing inducting heating to control the non-linearities in temperature measurement was used to control the heat transfer mechanism of SMA. Temperature-induced shape memory effect of Flexinol NiTi wire with preloads ranging from 5N to 25N were evaluated in terms of the phase transformation temperatures, thermal hysteresis and the generated strains. With increasing preloads, the phase transformation temperatures and transformation strain also increased, while the thermal hysteresis decreased. The strain-temperature curves during thermal loading at different loads demonstrated a prominent shape memory effect using induction heating. The experimental results signified that induction heating offer a regulated temperature control and faster heating capability, thus become a promising heating technique for SMA thermomechanical characterization.

Keywords: Shape memory alloy, Shape memory effect, Load, Temperature, Induction heating

I. INTRODUCTION

Nickel titanium (NiTi) is a commercially available shape memory alloy (SMA) that has two prominent functional properties which are shape memory effect (SME) and superelasticity (SE) [1,2]. Both reflects the ability of the material to restore deformation due to mechanical and thermal loading, respectively as a result of mutual reversible solid to solid thermoelastic transformation from martensite phase to austenite phase [3]. The martensite phase can exist in two variants namely twinned and detwinned martensite. The ability to produce restoring force and displacement promotes innovative design application of robot arms, adaptive wings, SMA embedded in concrete column, sensor, actuator and reinforced SMA composites [4]. Primary challenges on employing SMA as actuators mainly focus on controlling its nonlinear behaviour through regulated temperature control to ensure precise SMA thermomechanical characterization is attained [5]. Feasible heat activation integrated with applied stress and temperature is crucial to attain a reliable shape memory effect, thus achieving the desired actuation with stable hysteresis. Most reported work SMA characterization conduct temperature activation through electric heating such as Joule heating [6,7] and different cooling method such as natural air

Manuscript received, July 1, 2024, final revision, September 1, 2024
* To whom correspondence should be addressed, E-mail: dlaila@upm.edu.my

cooling [8], air cooling [9] and liquid cooling [10]. Both these factors resulted in irregular hysteresis shape due to improper temperature control [11], thus influences the phase transformation temperatures and transformation strain. Therefore, a reliable thermomechanical characterization via experimental approach using induction heating needs to be established in order to optimize the use of wire in actuator applications.

In this study, a commercial SMA wire produced by Dynalloy, Inc., USA, whose trade name is Flexinol was loaded from 5 N to 25 N using loading setup with dedicated enclosed heat control chamber and, comparing those results with those obtained by Differential Scanning Calorimetry (DSC) at zero preload (load free) condition. This step is to compare the phase transformation temperatures obtained from both methods. Since, data measurement is very crucial in macroscopic approach, a precise regulated heat control chamber to control the non-linearities in temperature measurement is paramount to loading setup. In this study, the effect of preloads on the observable properties such as phase transformation temperatures, thermal hysteresis and transformation strain were analysed. It can also compensate for the inaccuracy characterization developed via existing unregulated heating methods and therefore can provide more feasible heat control scheme and thus higher accuracy in the characterization of SMA response.

II. MATERIALS AND METHODS

2.1 Material

Nickel titanium wire alloys with 50% nickel and titanium compositions respectively were used in this study. This wire is commercially known as NiTi Flexinol made by Dynalloy, Inc., USA with a diameter of 0.3048 mm and can provide a maximum pull force of 25N as recommended by the manufacturer [12]. The wires were cut into length of 300 mm for the use as specimens in the experimental work as shown in Figure 1.

(a) Flexinol actuator wire roll

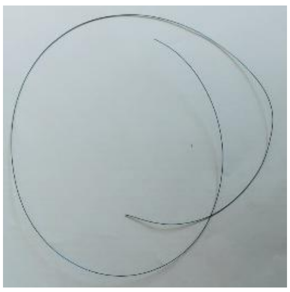

(b) Experimental sample of Flexinol actuator wire

Figure 1 Flexinol SMA actuator wire

2.2. Differential scanning calorimetry (DSC)

In this study, differential scanning calorimetry (DSC) test was carried out to determine the phase transformation temperatures of NiTi wire at zero preload condition. The peculiar responsive behaviour of wire at exothermic and endothermic peaks during the thermal cycle was observed in this test. A small piece of wire sample with 42.64 mg was cut out with 2 mm in height for DSC test. In this course of study, a Perkin Elmer Jade DSC equipment was used according to the ASTM standard [13]. The applied heating and cooling rate were 10°C/min respectively and the test was conducted between 0°C to 100 °C and held at 0°C and 100°C for 5 minutes respectively.

2.3. Experimental setup with induction heating

The effect of different preloads on the strain response of NiTi wire at different temperature levels were evaluated using a specially designed aluminium frame that accommodates the placement of the wire in a heat chamber and hanging dead weights at one end as shown in Figure 2. At the centre of the frame, a 300 mm length Flexinol wire is attached to a fixed base and extended upwards through movable frictionless roller which was fixed with load cells via spool grips. The preload was applied by hanging dead weights to the end of bearing and roller. The dead weight also acted as the bias force needed to stretch the SMA wire back to its original length when in the cooling cycle. The Flexinol wire went through a specifically designed heat control chamber with induction heating that is capable of providing a contactless and uniform temperature distribution along the length of the wire up and temperature can be controlled up to 0.01°C sensitivity. The temperature-induced cycle involved in heating from ambient to 90^{0}C and cooling at a constant rate of 5°C/min [14] for each preload. The frame was also instrumented with a load cell and laser displacement sensor to measure the force and displacement and readings are acquired using LabView with National Instrument Data Acquisition System (NI DAQ).

It is important to mention here that a specialized induction heating method that capable of providing uniform homogenous heating and cooling cycles with precise temperature control and contactless heating is the main contributing factor to the accuracy of the strain produced by the SMA wire. This chamber consists of an induction coil in which the SMA wire is inserted and an electromagnetic field is induced to generate heat in the wire. The drawbacks of the more common approach of Joule heating resulted in incorrect hysteresis size and shape which leads to inaccurate phase transformation temperatures. A feedback controller system is integrated with the chamber to regulate the temperature profile precisely. A user interface specifically programmed to control and monitor the temperature of specimen was used to measure the temperature data of wire and connected to heat chamber via Bluetooth connection. Discussion on the potential of induction heating system as a means of effective and homogenous heating method due to efficient heat transfer rate was also previously reported [15].

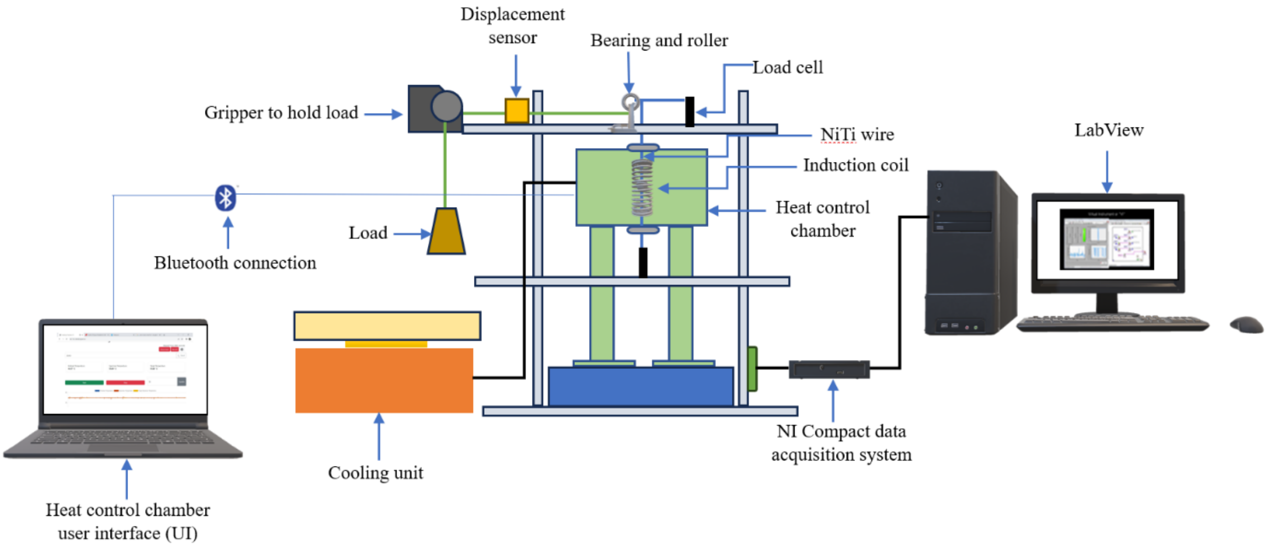

Figure 2 Experimental set-up for loading configuration with induction heating

2.4. Derivation of the typical features of SME from strain-temperature diagram

In this section, the derivation of the typical feature of SME from the strain-temperature diagram is demonstrated in Figure 3. The features are the amount of transformation strain, phase transformation temperature, thermal hysteresis and the irrecoverable strain if exists. The phase transformation temperature is the temperature required to induce the reorientation of the crystalline structure of Flexinol wire. The temperature difference between the heating and cooling cycles is represented as the thermal hysteresis [16]. The ideal equilibrium curve for hysteresis loop is defined as temperature difference of the material at 50% austenite transformation during heating cycle and 50% martensite transformation during cooling [16,17]

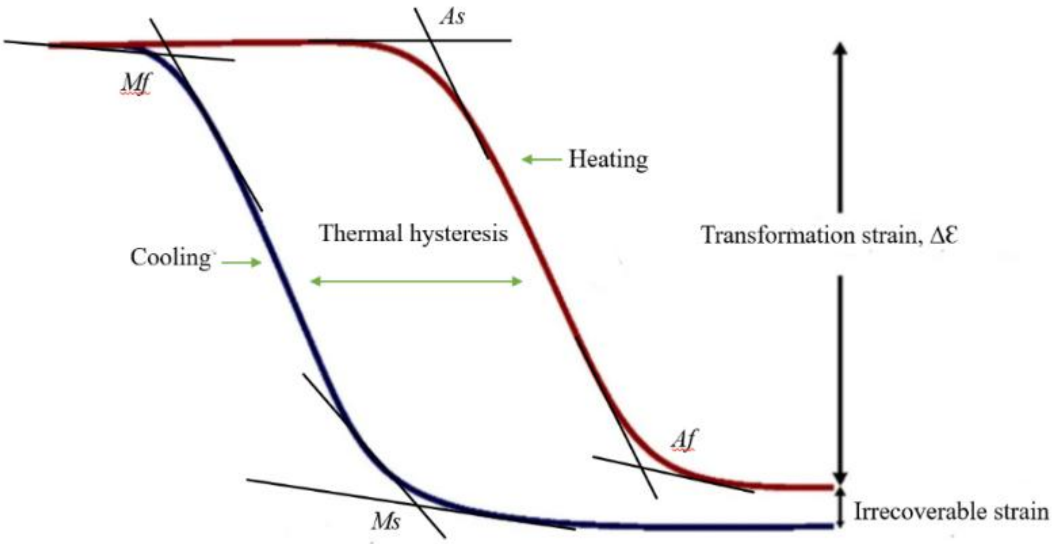

Figure 3 Typical features of SME [2]

III. RESULTS AND DISCUSSION

3.1 Phase transformation temperatures from DSC testing

In this study, the phase transformation temperature of Flexinol wire at zero preload is determined to identify at what temperature the wire is activated or induced for phase transformation without any preloads. The DSC curve in Figure 4 presented phase transformation temperatures of the wire with austenite start temperature, A_s = 82.37°C, austenite finish temperature, A_f= 89.08°C, martensite start temperature, M_s = 44.36°C, and martensite finish temperature, M_f = 32.14°C. The tangent lines constructed to each start and finish of each peak with reference to the baseline heat flows was used to determine the start and finish of each transformation.

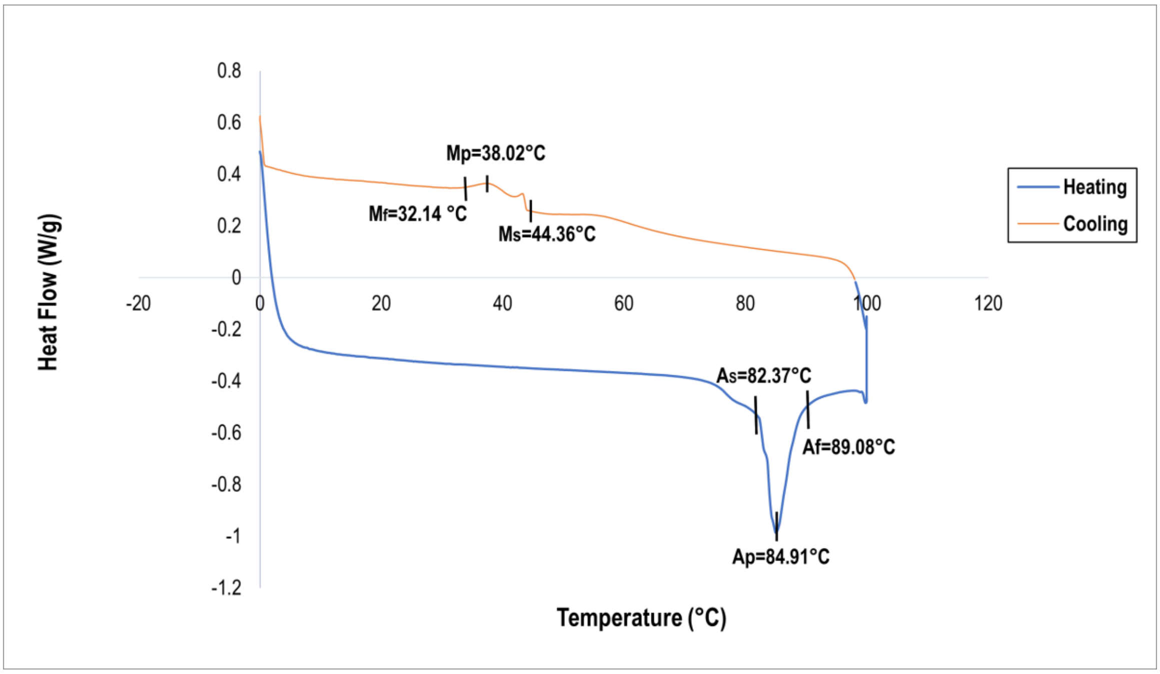

Figure 4 DSC results for NiTi Flexinol Wire

There were two exothermic peaks observed in Figure 4 upon cooling corresponding to the forward martensitic transformation. The transformation changes from cubic lattice known as B2-austenite into twinned martensite known as monoclinic B19'-martensite with martensite peak temperature of 38.02°C. There is presence of R-martensite transformation in between with peak temperature of 43.33°C. This is due to the contribution of the internal load which initiated the crystallographic lattice orientation [18]. However, upon heating there is only one endothermal peak corresponding to the reverse martensitic transformation from B19'-martensite to B2-austenite with peak temperature of 84.91°C. This implies that the internal loads stabilize during the reverse phase transformation. Herein, the discussion on the microstructure change is based on the similar reported works in Table 1.

Table 1 Phase Transformation Temperature of NiTi Flexinol Wire from Reported Works

Reported work	M_s (°C)	M_f (°C)	A_s (°C)	A_f (°C)
Current work	44.36	32.14	82.37	89.08
Danish et. al. [19]	36.12	25.26	74.59	81.62
Granberry et al [20]	42.0	25.5	66.0	76.5
Abdelaal [21]	52	42	68	78
Potapov et.al [22]	44	26	59	75

The material states of the wire in Figure 4 depicts the phase transformation temperatures at zero preloads, which will be referred as baseline values when preloading is introduced. Herein, the DSC result does not give accurate and reliable prediction of real-time phase transformation temperatures that is dynamic in nature due to the existence of variations in loading and temperature.

Table 2 Comparisons of Testing Parameters of NiTi Flexinol Wire from Reported Works

Reported work	Sample size	Temperature range
Current work	42.64 mg	0°C to 100°C
Danish et. al. [20]	27.5mg	-
Granberry et al [21]	-	-125 °C to 125 °C
Abdelaal [22]	-	20 °C to 115 °C

Table 1 outlined the inconsistencies of the DSC results with similar reported works that also established the phase transformations for Flexinol in accordance to the same standard testing method. The comparison of current DSC results with the average of other published works shows 1.87% in M_s, 7.6% in M_f, 18.78% in A_s and 12.69% in A_f percentage differences in the transformation phases. This might due to different annealing rate, different holding time, material composition, location of sensors and processing conditions (which in this case is the same) as well as sample mass and temperature range as outlined in Table 2. However, DSC method based on established standard like ASTM F2004-05 is still considered a valuable tool for purpose of material screening. The influential factors were specified in certain range of values in the standard, thus resulting in the inconsistencies in the transformation temperatures. For example, the mass of specimen stated in the standard is between 20 mg to 50 mg, which varies the total surface area of specimen and affect the heat absorption and heat release by the specimen. This implied that the associated influential factors discussed above were not clearly explained or described in the ASTM F2004-05, thus reduce the accuracy and precession of DSC results for similar material. Therefore, a viable experimental method employing loading setup connected with induction heating method to measure phase transformation temperature is explained in the next section.

3.2 Phase transformation temperature at different preloads

SME in this section is described as the complete cycle of the contraction of wire with heating and extension of wire with cooling. When the preload is increased, the relationship between the strain amplitude and phase transformation cycle is shown in the Figure 5. There is a significant upward shift in strain amplitude and distinguished right shift in phase transformation temperature with increasing preloads. This means that the deformation ability of Flexinol wire increases continuously during the thermal cycle, and could provide enough strain response to restore the deformation at different applied preloads. The increasing of preloads varies the shift of the SME loop which is associated with phase transformation temperatures.

Results in Table 3 showed that with increasing preloads, all four phase transformation temperatures increase as well. Increasing preloads increases the strain and the resultant storage energy. Therefore, more time is required by the wire to be activated in order to induce the phase transformation occurrences with the presence of preloads. This also implies that more heat energy is required to induce the activation states of the wire which was deformed by the preloads. This thermal cyclic phenomenon is due to the orientation of the crystalline lattice structure [23] of Flexinol wire that varies differently during the heating and cooling phase with the presence of preloads [24]. However, compared to the DCS result for zero preloads, the trend in Table 3 shows that the martensitic phase transformation temperatures increasing with increasing preloads, whereas the austenitic phase transformation temperatures decreasing with increasing preloads. For this observation, it was anticipated that the presence of preloads might decrease the build-up and storage of elastic energy [25], thus requires less heat energy to induce the activation states of the wire [26].

To put this shift of phase transformation temperature together into perspective with the presence of preloads, a trendline for the result presented in Table 3 is constructed as shown in Figure 6. It highlights the relative correlation of phase transformation temperature with the increment of preloads. Note that the change on the phase transformation temperatures is approximately less than 1°C for every 1 N increment. At a maximum of 25 N preload, the change in phase transformation temperatures is between 10 to 16^0 C. The changes will directly affect the size of the hysteresis loop that is critical to determine the generated actuation strain. The linear trendline can be extended to cross the yaxis for the determination of the phase transformation temperature at zero preload which is also reported in Table 1. In comparison to the DSC results, the zero preload results obtained via hysteresis is significantly lower for the austenite transformation temperatures. This could be due the higher stored elastic strain energy [27] which resulted faster initiation of reverse transformation due to less heating [28]. In addition, the trend associated to the change in austenitic temperatures with the increasing applied load is indefinite. Therefore, given the disparity in phase transformation temperatures provided by DSC test, the experimental methods with induction heating in this study would be required to understand interplay between phase transformation temperatures and other transformation properties.

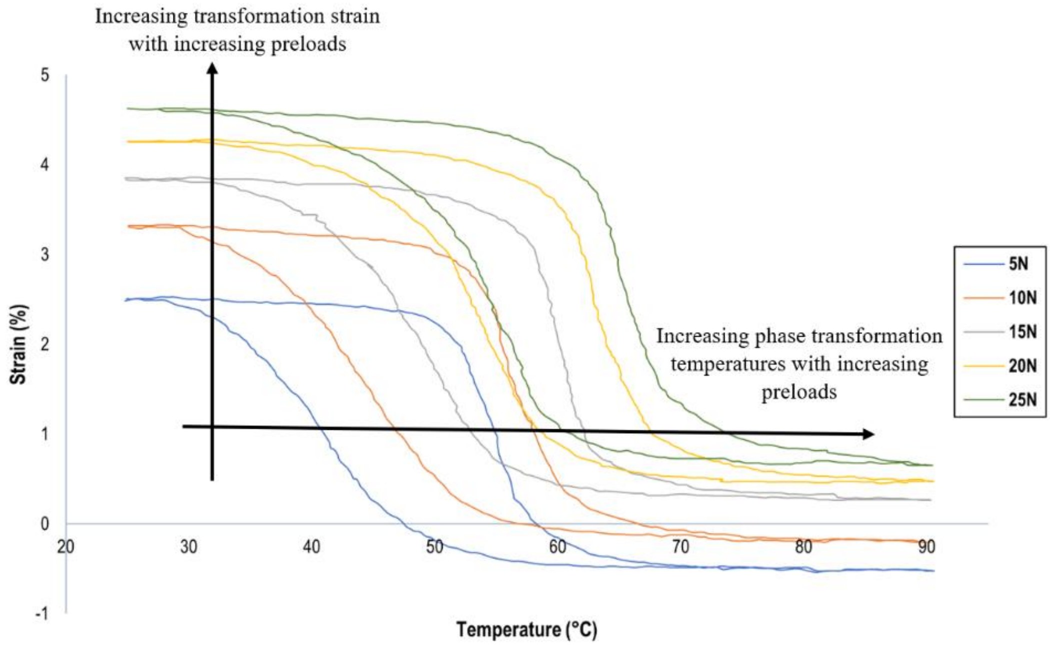

Figure 5 SME Behaviour of NiTi Flexinol Wire at Different Preloads

Table 3 Phase transformation temperature of NiTi Flexinol wire

Load (N)	Ms (°C)	Mf (°C)	As (°C)	Af (°C)
0 (extrapolated)	44.4	28	46.4	57
5	48	34	50	60
10	50	36	52	62
15	54	38	56	64
20	58	48	60	68
25	60	50	62	70

3.3 Effect of different preloads on the thermal hysteresis

The transformation strain which refers to the actuation length or amount of stroke produced in the wire may be critical information required to ensure the feasibility of wire for a given engineering application. In this section, the effect of preloads on the thermal hysteresis and the amount of strain generated are presented in Figure 7. Herein, the similarity in the shape of the hysteresis for all preloads that strongly suggest the effectiveness of the heating and cooling using induction method.

The shape of the thermal loops for all the different preloads were similar with Δ T gradually decreasing from 14.4°C to 9.5°C as shown in Figure 7 with increasing preloads. The gradual decrease is associated with total change in martensitic and austenitic phase transformation loops. Note that in the Table 4, the change in martensite loop is greater than the change in austenitic loop with increasing preloads. This indicates that the greater change in martensite loop might due to the dissipation of stored elastic energy during forward transformation caused by plastic deformation [24]. For the reverse transformation, it is smaller due to the build-up and storage of elastic strain energy which decrease with increasing preloads [24,25]. The presence of preloads further increases the amount of heat dissipated in martensitic loop and decreases the amount of heat absorbed in austenitic loop. This phenomenon narrowed the width of the thermal hysteresis loop, thus increase the amount of stroke generated by the wire. Besides that, the thermal hysteresis for all the preloads were close loops with no permanent residual strain. This is because the strain generation is within the yield strength of the wire. Therefore, in practical actuator application, it is recommended that preloads are introduced with the nature of preloads must be below the yield strength of wire so that it does not change the length.

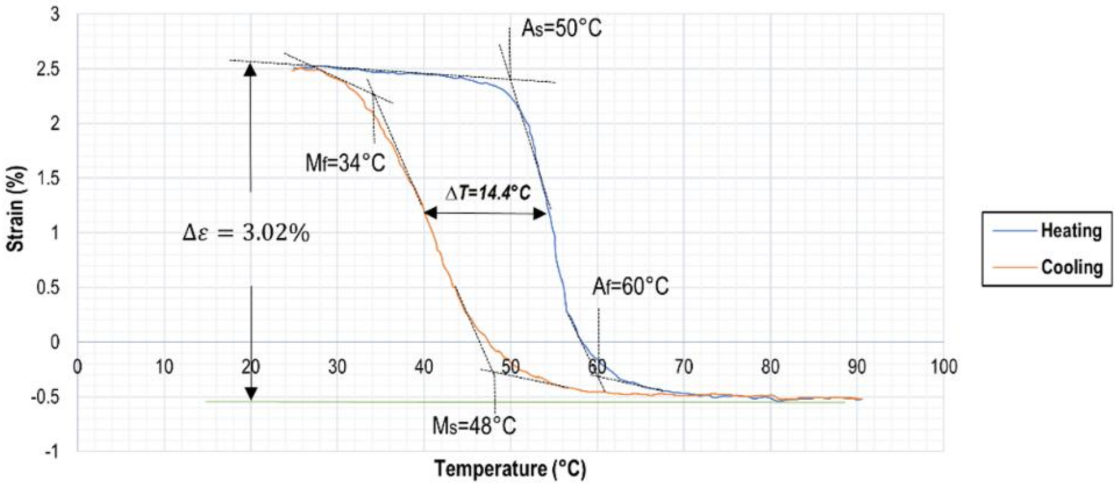

(a) 5N

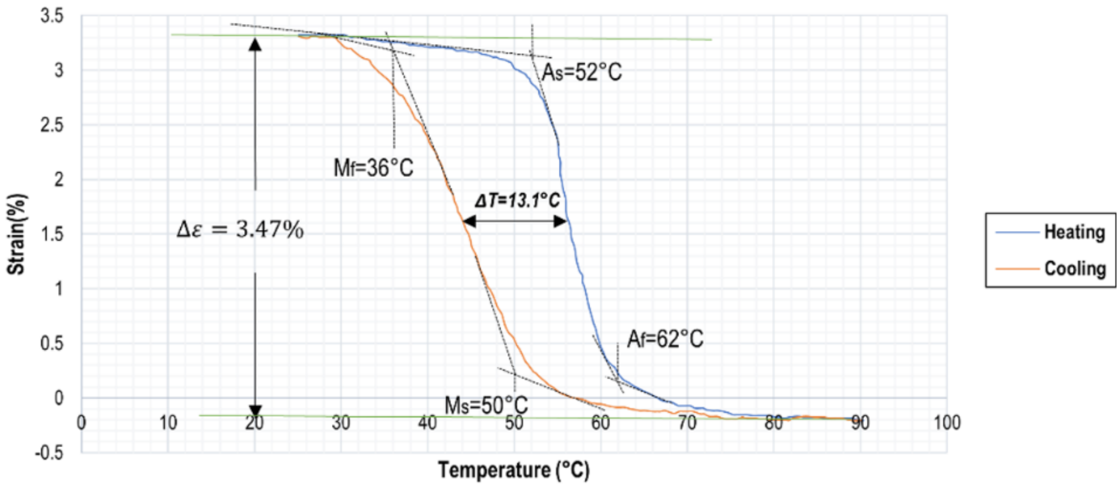

(b) 10N

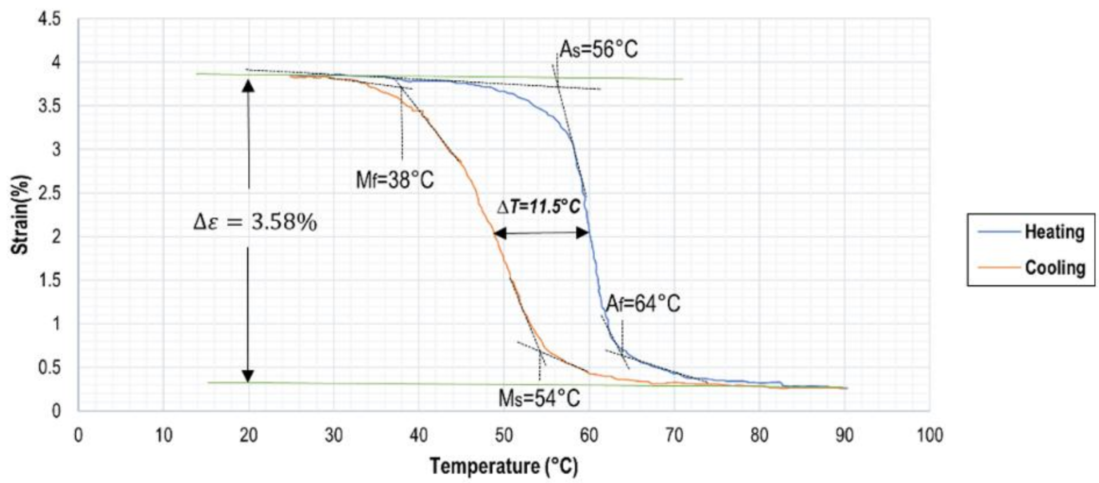

(c) 15N

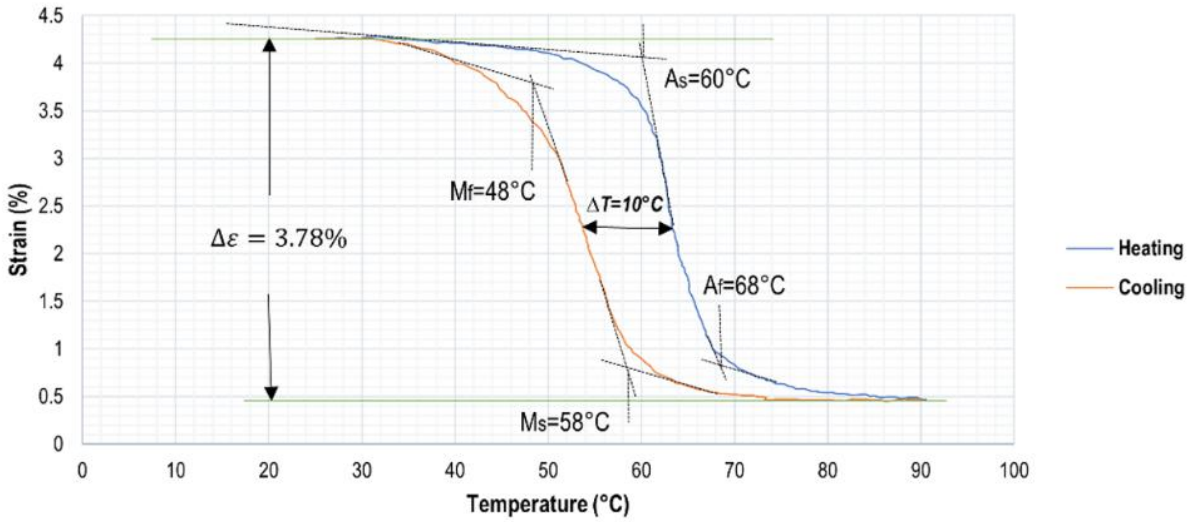

(d) 20N

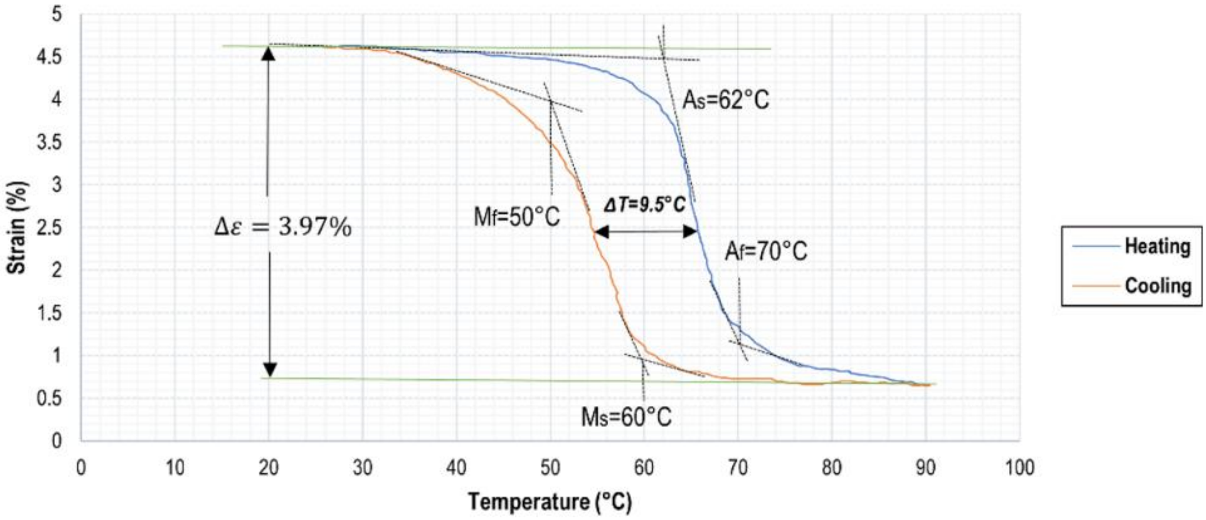

(e) 25N

Figure 7 Phase Transformation Temperatures of NiTi Wire at Different Preloads

Table 4 Thermal hysteresis and transformation strain of NiTi Flexinol wire

Weight (N)	ΔT_F (°C)	ΔT_R (°C)	Hysteresis (°C)	Strain (%)
5	14.00	10.00	14.40	3.02
10	14.00	10.00	13.10	3.47
15	16.00	8.00	11.50	3.58
20	10.00	8.00	10.00	3.78
25	10.00	8.00	9.50	3.97

The relationship between the thermal hysteresis and amount of strain generated is shown in Figure 8. The amount of stroke generated by the wire is inversely proportional with the thermal hysteresis with increasing preloads. This trend is associated with the change in the dislocation loops of the phase transformation. Dislocation of loops is propagated by the elastic stored energy within the interface loops [28] resulting in the generation of strain by wire [29]. This propagation further modifies the internal load of wire within the loops by energy absorption and energy dissipation. In this study, the increase in energy dissipation increases the internal load in martensitic loop, whereas, the decrease in energy absorption decreases the internal load of the wire in austenitic loop. These changes narrowed the hysteresis loop [25] and increases the amount of stroke generated by the wire during the thermal cycle [27].

Herein, a smaller thermal hysteresis is critical requirement for actuator design as it influences the response time and frequency actuator [30]. This inverse relation implies that higher preload is favourable to optimize the stroke generated. Close study of strain-temperature curve for SMA wire subjected to thermal cycle and preloads reveals that the variation of transformation temperatures with increment of preloads significantly influences the strain response in the shape memory effect behaviour of SMA wire which is critical especially for actuation applications. Table 5 shows the comparison of maximum attainable stroke of established study with other heating methods. The maximum attainable stroke is almost 4% using induction heating and this is also suggested by Dynalloy Inc. in the technical note of the Flexinol wire that further reinforced the reliability of the test method adopted in the current work. On contrary, other heating techniques exhibited less than 4% maximum stroke and strongly implied that inaccurate actuation obtained due to the improper temperature control, thus resulting in incorrect hysteresis size and shape.

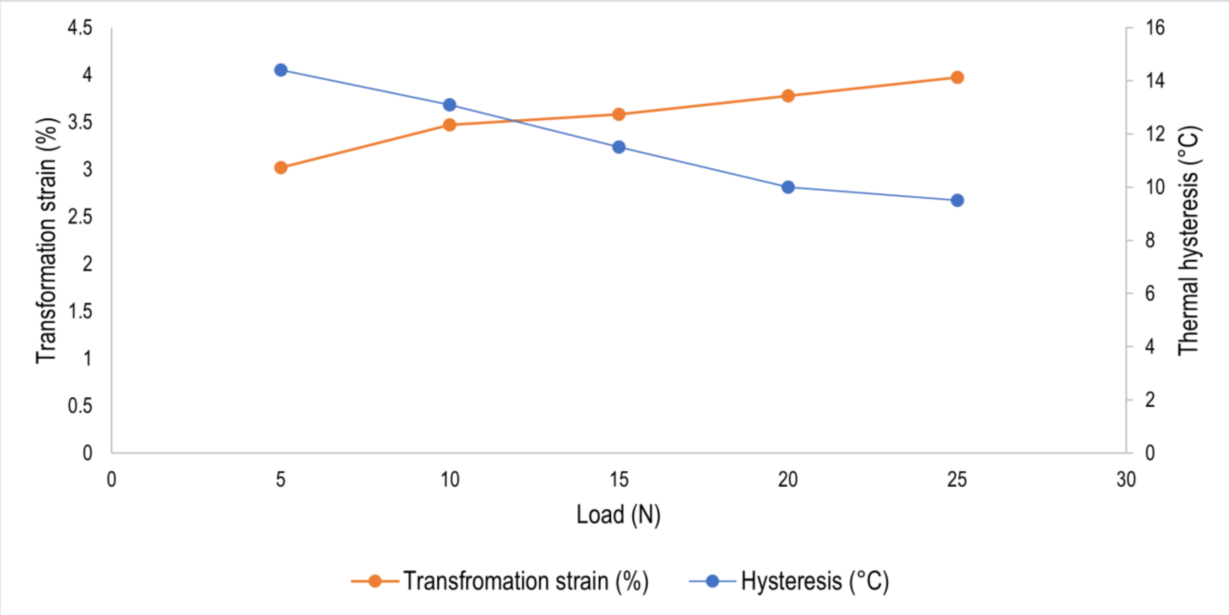

Figure 8 Relationship between Thermal Hysteresis and Transformation Strain

Table 5 Comparison of maximum attainable stroke with other heating techniques

Heating methods	Maximum transformation strain (%)
Induction heating (current study)	4.0
Joule heating [31]	2.0
Electrical heating [32]	3.0
Hot water/liquid [33]	2.5

In conclusions, induction heating method capable to actuate SMA wire accurately depending on the desired applications. In many applications, the actuator wire in structural elements probably will undergo dynamic loadings, requiring an accurate yet practical estimation of the effect of preloads on the performance and functionality of the actuator for long term use. Even though the stroke does not undergo a large change due to the preload, but the significant shift in activation temperatures requires changes to be made in the setting of the targeted activation temperature of the actuator. Therefore, with the application of feasible and regulated induction heating method, a precise actuation is achieved.

IV. CONCLUSIONS

In this study, the reliability of the induction heating is demonstrated via the resultant similar shaped hysteresis that were obtained from the thermal cycles of various preloading. The effectiveness of heating and cooling by induction heating is proven through the prominent hysteresis shape and well-established trend of the phase transformation temperature and load. The phase transformation obtained with DSC in zero stress condition is different compared to the one obtained with the presence of preloads due to influential factors such as material composition and processing conditions, location of sensors, sample mass and temperature range. This led to inaccurate prediction of phase transformation temperatures in practical dynamic condition. Besides that, it was shown that the phase transformation temperature increases with increasing preloads. Conversely, with increasing preloads, the thermal hysteresis is inversely proportional to the transformation strain. This influences the stroke generation of SMA wire which is a critical information for designing an actuator for given engineering application.

ACKNOWLEDGMENTS

The authors would like to acknowledge the financial support from the Ministry of Higher Education under the Fundamental Research Grant Scheme with grant no. FRGS/1/2019/STG07/UPM/02/10.

REFERENCES

[1] Costanza G, Tata ME, Libertini R, "Effect of Temperature on the Mechanical Behaviour of Ni-Ti Shape Memory Sheet," In: TMS 145th Annual Meeting & Exhibition. Springer, Cham, 2016. https://doi.org/10.1007/978-3-319-48254-5_52

[2] Jani JM, Leary M, Subic A, Gibson MA, "A review of shape memory alloy research, applications and opportunities," *Materials & Design*, Vol. 56, 2014, pp. 1078-1113. https://doi.org/10.1016/j.matdes.2013.11.084

[3] Han F, Wong MB, Bai Y, Luo R. "Effect of heating/cooling rates on the material properties of NiTi wires for civil structural applications," *Construction and Building Materials*, Vol.101, No.1, 2015, pp. 447-455. https://doi.org/10.1016/j.conbuildmat.2015.10.081

[4] Shokuhfar A, Khalili SMR, Ghasemi FA, Malekzadeh K, Raissi S. "Analysis and optimization of smart hybrid composite plates subjected to low-velocity impact using the response surface methodology (RSM)," *Thin-Walled Structures*, Vol. 46, No.11, 2008, pp. 1204-1212. https://doi.org/10.1016/j.tws.2008.02.007

[5] Luji FFJ, Teo KT, Tan SF, Yoong HP, "Heating and Cooling Mechanisms for SMA Actuator - A Brief Review," *Transactions on Science and Technology*, Vol.8, 2021, pp. 425-431. https://doi.org/10.1109/TTHZ.2018.2886942

[6] Wada K, Liu Y, "Shape recovery of NiTi shape memory alloy under various pre-strain and constraint conditions," *Smart Materials and Structures*, Vol. 14, No. 5, 2005, pp. 273-S286. https://doi.org/10.1088/0964-1726/14/5/016

[7] Vitiello A, Giorleo G, Morace RE, "Analysis of thermomechanical behaviour of Nitinol wires with high strain rates," *Smart Materials and Structures*, Vol. 14, No. 1, 2004, pp. 215-221. https://doi.org/10.1088/0964-1726/14/1/021

[8] Kim Y, Taesoo J, Hema G, Mansour NA, Bongjo R, Buhyun S. "Bidirectional rotating actuators using shape memory alloy wires," *Sensors and Actuators A: Physical*, Vol. 295, 2019, pp. 512-522 https://doi.org/10.1016/j.sna.2019.05.047

[9] Taylor F, Au C, "Forced air cooling of shape-memory alloy actuators for a prosthetic hand," *Journal of Computing and Information Science in Engineering*, Vol. 16, No. 4, 2016, pp. 041004. https://doi.org/10.1115/1.4033233

[10] Peng C, Yin YH, Hong HB, Zhang JJ, Cheng X, "Bio-inspired design methodology of sensor-actuator-structure integrated system for artificial muscle using SMA," *Procedia CIRP*, Vol. 65, 2017, pp. 299-303. https://doi.org/10.1016/j.procir.2017.04.016

[11] Choon TW, Salleh AS, Jamian S, Ghazali MI, "Phase Transformation Temperatures for Shape Memory Alloy Wire," *World Academy of Science, Engineering and Technology,* Vol. 25, 2007, pp. 304-307. https://zenodo.org/record/1081669

[12] DYNALLOY, Inc. (2024). Technical Characteristics of Flexinol [Actuator Wires]. Retrieved from https://www.dynalloy.com/tech_data_wire.php

[13] ASTM F2004-05. Standard test method for transformation temperature of nickel–titanium alloys by thermal analysis. West Conshohocken, PA, USA: ASTM International; 2010. https://www.astm.org/f2004-03.html

[14] Asl FJ, Kadkhodaei M, Karimzadeh F, "The effects of shape-setting on transformation temperatures of pseudoelastic shape memory alloy springs," *Journal of Science: Advanced Materials and Devices*, Vol. 4, No. 4, 2019, pp. 568-576. https://doi.org/10.1016/j.jsamd.2019.10.005

[15] Karunakaran S, Majid DLAA, Jaafar CNA, Ismail MH, Imran HY, "Heating Techniques of Shape Memory Alloy (SMA) - A Review," *Journal of Advanced Research in Fluid Mechanics and Thermal Sciences*, Vol. 99, No. 2, 2022, pp. 207-220. https://doi.org/10.37934/arfmts.99.2.207220

[16] Reynold DR, "A Nonlinear Thermodynamic Model for Phase Transitions in Shape Memory Alloy Wire," Doctoral dissertation, Southern Methodist University, 2003. http://hdl.handle.net/1911/18602

[17] Lagoudas D, Hartl D, Chemisky Y, Machado L, Popov P, "Constitutive model for the numerical analysis of phase transformation in polycrystalline shape memory alloys," *International Journal of Plasticity*, Vol.32, 2012, pp. 155-183. https://doi.org/10.1016/j.ijplas.2011.10.009

[18] Otsuka K, Wayman CM, (Eds.), Shape Memory Materials, Cambridge Univ. Press, Cambridge, 1998. https://link.springer.com/article/10.1557/S0883769400037350

[19] Baitab DM, Majid DL, Abdullaha ER, Hamid MF, "Tensile behavior of multilayer 3D smart woven composites embedded with shape memory alloy (SMA) wires," *Journal of Materials Research and Technology*, Vol. 9, No. 5, 2020, pp. 10876-10885. https://doi.org/10.1016/j.jmrt.2020.07.035

[20] Granberry R, Eschen K, Holschuh B, Abel J, "Functionally Graded Knitted Actuators with NiTi - Based Shape Memory Alloys for Topographically Self - Fitting Wearables," *Advanced Materials Technologies*, 2019, pp. 1900548. https://doi.org/10.1002/admt.201900548

[21] Abdelaal WGA, Nagib G, "Modeling and simulation of SMA actuator wire," 9th International Conference on Computer Engineering & Systems (ICCES), Cairo, 2014, pp. 401-405.

https://doi.org/10.1109/ICCES.2014.7030993

[22] Potapov PL, Da Silva EP, "Time Response of Shape Memory Alloy Actuators," *Journal of Intelligent Material Systems and Structures*, Vol. 11, No. 2, 2000, pp. 125-134. https://doi.org/10.1106/XH1H-FH3Q-1YEX-4H3F

[23] Barbarino S, Flores EIS, Ajaj RM, Dayyani I, Friswell MI, "A review on shape memory alloys with applications to morphing aircraft," *Smart Material Structure*, Vol. 23, 2014, pp. 1-19. https://doi.org/10.1088/0964-1726/23/6/063001

[24] Hamilton RF, Lanba A, Ozbulut OE, et al. "Shape Memory Effect in Cast Versus Deformation-Processed NiTiNb Alloys," *Shap. Mem. Superelasticity*, Vol.1, 2015, pp.117-123. https://doi.org/10.1007/s40830-015-0024-1

[25] Ortin J, Delaey L, "Hysteresis in shape-memory alloys," *International Journal of Non-linear Mechanics*, Vol. 37, 2002, pp. 1275-1281. https://doi.org/10.1016/S0020-7462(02)00027-6

[26] Sehitoglu H, Hamilton R, Maier HJ, Chumlyakov Y, "Hysteresis in NiTi alloys," *J. Phys*. IV France, Vol. 115, 2004, pp. 3-10. https://doi.org/10.1051/jp4:2004115001

[27] Hamilton RF, Sehitoglu H, Chumlyakov Y, "Stress dependence of the hysteresis in single crystal NiTi alloys," *Acta Materialia*, Vol. 52, No. 11, 2004, pp. 3383-3402. https://doi.org/10.1016/j.actamat.2004.03.038

[28] Lemke JN, Coda A, "DSC and microstructure analysis of high temperature Ni-Ti-Hf, low hysteresis Ni-Ti-Cu and conventional super-elastic and shape memory Ni-Ti alloy," *Materials Today Communications*, Vol. 21, 2019, pp.10066. https://doi.org/10.1016/j.mtcomm.2019.100666

[29] Malukhin K, Ehmann K, "A model of the kinetics of the temperature-induced phase transformation in NiTi alloys and its experimental verification," *Journal of Intelligent Material Systems and Structures*. Vol. 23, No. 1, 2012, pp. 35-44. https://doi.org/10.1177/1045389X11430728

[30] Reynold DR, "A Nonlinear Thermodynamic Model for Phase Transitions in Shape Memory Alloy Wire," Doctoral dissertation, Southern Methodist University, 2003. https://hdl.handle.net/1911/18602.

[31] Furst SJ, Seelecke S. "Modeling and experimental characterization of the stress, strain, and resistance of shape memory alloy actuator wires with controlled power input," *Journal of Intelligent Material Systems and Structures*, Vol. 23, No. 11, 2012, pp. 1233-1247. https://doi.org/10.1177/1045389X12445036

[32] Tadesse Y, Thayer N, Priya S. "Tailoring the Response Time of Shape Memory Alloy Wires through Active Cooling and Pre-stress," *Journal of Intelligent Material Systems and Structures,* Vol. 21, No. 1, 2010, pp. 19-40. https://doi.org/10.1177/1045389X09352814

[33] Sagar SNK, Sreekumar M, "Miniaturized Flexible Flow Pump Using SMA Actuator," *Procedia Engineering*, Vol. 64, 2013, pp. 896-906. https://doi.org/10.1016/j.proeng.2013.09.166